Wavelet Analysis of Poorly-Focused Ultrasonic Signal of Pressure Tube Inspection in Nuclear Industry

Huan Zhao, Anthony Gachagan, Gordon Dobie and Timothy Lardner

Centre for Ultrasonic Engineering, University of Strathclyde, Glasgow, UK

Corresponding author: huan.zhao@strath.ac.uk

Abstract. Pressure tube fabrication and installment challenges combined with natural sagging over time can produce issues with probe alignment for pressure tube inspection of the primary circuit of CANDU reactors. The ability to extract accurate defect depth information from poorly-focused ultrasonic signals would reduce additional inspection procedures, which leads to a significant time and cost saving. Currently, the defect depth measurement protocol is to simply calculate the time difference between the peaks of the echo signals from the tube surface and the defect from a single element probe focused at the back-wall depth. When alignment issues are present, incorrect focusing results in interference within the returning echo signal. This paper proposes a novel wavelet analysis method that employs the Haar wavelet to decompose the original poorly focused A-scan signal and reconstruct detailed information based on a selected high frequency component range within the bandwidth of the transducer. Compared to the original signal, the wavelet analysis method provides additional characteristic defect information and an improved estimate of defect depth with errors less than 5%.

1. INTRODUCTION

Pressure tubes ultized within the CANDU (CANada Deuterium Uranium) nuclear reactor are used for natural uranium operation with D_2O moderator. The inspection of pressure tubes is important to prevent malfunctioning tubes from influencing the electrical power supply. Ultrasonic technology is utilized to inspect the 4.3 mm thick zirconium – niobium tube walls for precise size measurement of features and defects [1]. Currently, single element focused transducers are employed to detect defects and ascertain their geometric characteristic. However, due to the fabrication and installment challenges combined with natural sagging over time, transducer alignment can be problematic during the tube inspection and result in reduced accuracy of the inspection. Following the inspection process, if the measured depth is larger than a predefined threshold, a replica process should be executed to produce a high accuracy measurement of the defect depth to aid the safety case. Importantly, this additional process is costly in terms of time and finance, and results in additional dosage for inspection technicians. Any reduction in the accuracy of the ultrasonic inspection has a direct correlation with an increase in the number of replica required. Therefore, extracting precise defect depth information from the poorly-focused ultrasonic signals becomes particularly important.

A detailed examination of the signal processing to enhance poorly focused ultrasonic data has not been applied to the problem. Most of the solutions involve adjusting the scanning mechanics. In terms of the pressure tube inspection, the ultrasonic transducer is fixed on a module inside of the tube and moved with a helical scan motion. Therefore, it is not straight-forward to mechanically adjust the transducer position to solve the focusing problem. Using signal processing to extract useful information would be a more practical method. Taking advantage of the information beyond the focal point of a single element transducer has been investigated by some researchers. Frazier et al. proposed to take the focus of the transducer as a virtual source to apply SAFT (Synthetic Aperture Focusing Technique) on B-scan imaging data [2]. Wuest et al. carried forward the implementation of a virtual SAFT source for acoustic microscopy [3]. These methods provided a good use of the signal information beyond the focal point in the time domain and thus SAFT could be employed to improve the inspection resolution. However, in order to obtain superior results, the features of interest should ideally be located a large distance beyond the focus. Moreover, these methods mainly enhance the lateral resolution of the inspection.

Analyzing signals in frequency domain can be a useful way to characterize the behavior of the ultrasonic inspection. The Fourier Transform is a foundation of many signal processing algorithms in the frequency domain. Her and Lin introduced a frequency analysis concept to evaluate the depth of surface cracks [4]. According to their research, the time difference could be deduced from the frequency spectrum associated with the bottom surface crack. Short Time Fourier Transform (STFT) is one of the earliest applications for time-frequency analysis. Sharma et al. made use of STFT combined with an optimized window length to analyze the scattering from large grain sizes within a components microstructure, which reduced the high attenuation problem associated with measurements of highly scattering material [5]. The Split Spectrum Processing (SSP) technique had been utilized to improve the signal-noise-ratio (SNR) of coarse-grained materials inspection based on the frequency diversity [6]. An adaptive SSP algorithm was proposed by Bouden et al. based on an empirical method to analyze nonlinear and non-stationary signals, and perform recombination. This approach demonstrated a better extraction of defect information when compared to conventional SSP [7]. An analytical method to test acoustic wavefield images in frequency-wavenumber domain was presented by Ruzzene [8] and Michaels et al.[9]. This method increased the detection of weaker damage signals in a composite plate through removal of the incident wave.

Wavelet analysis has been widely used in ultrasonic Non-Destructive Testing (NDT) for SNR enhancement [10], weak defect signals extraction [11] and flaw signal classification [12]. This approach has demonstrated excellent improvement in identifying target signals by extracting signal features in the frequency domain, whilst maintaining the temporal information. However, to date, wavelets have mainly focused on signals in the low frequency regime. In this study, wavelet analysis of ultrasonic signals will focus in the high frequency level regime (10-20MHz) to enhance the extraction of the defect echo characteristics associated with pressure tube inspection. This paper is organized as follows: the methodology of the wavelet analysis is described in Section 2; the analysis of field data is introduced in Section 3; and Section 4 demonstrates the analysis results and discussion.

2. METHODOLOGY

2.1 Problem Definition

In situations when the ultrasonic inspection of CANDU pressure tubes produces poorly focused images of the tube surface, it results in difficulties to precisely measure the defect depth from the superimposed A-scan echo signals [1]. The A-scan signals acquired by an inspection tool CIGAR (Channel Inspection and Gauging Apparatus for Reactors) considered in this work are from a 15MHz normal beam used for detection of outer diameter flaws. To match the stringent requirements for the depth measurement accuracy (minimum defect depth size of 0.1 mm), conventional frequency analysis, such as STFT, does not produce sufficient accuracy due to the tradeoff between the time and frequency resolution. Hence, wavelet analysis is proposed here as a potential solution, based on its excellent performance to give combined information in frequency and time domains.

2.2 Wavelet Analysis

The wavelet transform is an analysis method to segment data into different frequency ranges and investigate each frequency component using corresponding time information. The operation involves two variables - frequency and time, which offers an efficient tool for time-frequency localization [13]. The primary difference between the wavelet transform and STFT is that the former has an adaptive frequency resolution as opposed to the uniform resolution associated with the latter. A description of the wavelet transform of a given function $f(t)$ can be expressed by

$$WT(a,b) = \frac{1}{\sqrt{a}} \int_{-\infty}^{+\infty} f(t) \cdot \psi\left(\frac{t-b}{a}\right) dt \tag{1}$$

where the functions $\psi_{a,b}$ are called wavelets,

$$\psi_{a,b}(\mathrm{s}) = \frac{1}{\sqrt{a}} \psi\left(\frac{s-b}{a}\right) \tag{2}$$

and the function ψ is called mother wavelet. Values a and b are the scale and shift parameters respectively. Here, we assume that the mother wavelet ψ satisfies the condition

$$\int_{-\infty}^{+\infty} \psi(t)\, dt = 0 \tag{3}$$

When parameter a changes, the wavelet function will address different frequency ranges and parameter b relates to the spectral movement of the wavelets. By applying different parameter values, the output of the wavelet transform is a series of coefficients related to the different frequency ranges. Thus a signal is decomposed into approximations (A) and details (D) on different levels according to frequency. A indicates the low frequency component, while D indicates the high frequency component. The signal S can be decomposed into n levels and can be expressed by

$$S = A_n + \sum_{j=1}^{n} D_j \tag{4}$$

where j is an integer.

The ultrasonic echo signal received from the pressure tube inspection is a high frequency signal, exhibiting low levels of noise. The detail signal for the wavelet analysis is reconstructed using these acquired ultrasonic echoes and used for defect observation within an appropriate frequency range. The decomposition of Discrete Wavelet Transform (DWT) operation in MATLAB (The MathWorks Inc., Natick, MA) can be found in FIGURE 1. For decomposition on more levels, a tree model is shown in FIGURE 2. The detail signal can be reconstructed directly from the wavelet coefficients on any level.

Considering the uncertainty principle of signal processing, the selection of the wavelet for the poorly-focused A-scan signal is more likely to have a high time resolution. As the simplest known orthonormal wavelets, Haar wavelets have extremely good time resolution, which should contribute to accurate time information for the extracted defect echo signal.

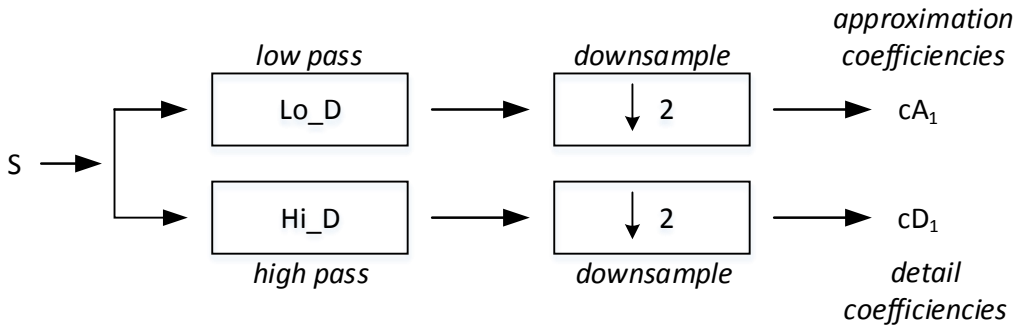

FIGURE 1. Process of decomposition of DWT in MATLAB

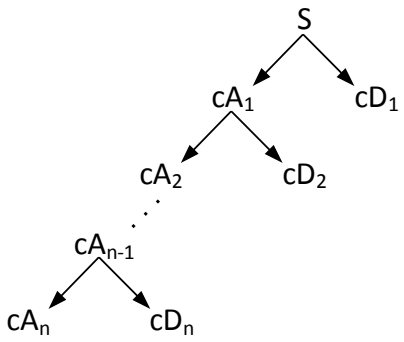

FIGURE 2. Tree model of a n-level wavelet decomposition

3. ANALYSIS OF INDUSTRIAL DATA

3.1 Data Acquisition

The sensor head, CIGAR, is employed to inspect the pressure tubes by executing a helical scan immersed in heavy water inside of the tubes. The ultrasonic inspection system experiences high damping, which results in a filtering effect of the center frequency of the received echoes from the 15MHz excitation frequency, as shown in FIGURE 3. Nevertheless, in a standard operation the time difference between the peaks in the received pulse-echo signals from the measured tube inner surface (no defect case) and the echo from the bottom of the defect is used to calculate the defect depth.

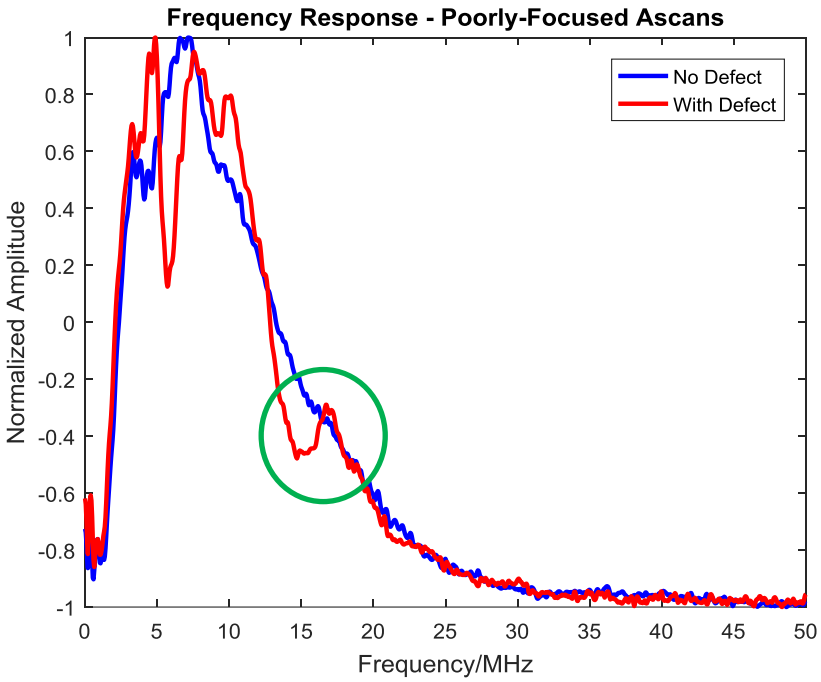

FIGURE 3. Frequency response from typical A-scan signals

3.2 Defect Depth Measurement in Flaw

A software analysis package, FLAW, is used to analyze CIGAR data and one function is specific to defect depth measurement. Initially, the acquired ultrasonic signal is presented as a B-scan image. Due to the movement during the helical scan, a wave straightening function, within FLAW, is typically applied to align the B-scan image, with the B-Scan image presented to the NDE Analyst as shown in FIGURE 4. This is an example of well-focused ultrasonic signal. The Analyst will select the most relevant A-scan signal (Signal 1) to measure the defect depth and another A-scan signal not containing defect information (Signal 0) is selected to represent the image backwall and used as a reference. The defect depth can be obtained through the time difference of the two peaks in the A-scan data also presented in the Figure.

In terms of the inspection configuration, the transducer focal length is 12.7 mm and the wave velocity in heavy water is 1420 m/s. For the inspection of the tube surface, the propagation time to reach the tube surface should be between 17.5-18μs. However, for a poorly-focused B-scan image, this time can be extended. Taking the inspection data in FIGURE 5 as an example, the time of ultrasonic wave reaching the tube surface is greater than the expected time and the defect echo signal is difficult to clearly identify from both the A-Scan and B-Scan associated with Signal 1, due to the superposition of the scatterings from the defect bottom and the defect edge near the tube surface.

3.3 Wavelet Processing

A-scan signals from this inspection have spectral characteristics, as shown in FIGURE 3 for two regions associated with the inner surface of the tube with and without the presence of a defect. These spectra are the average from a number of ultrasonic echo signals identified as belonging to either category. Each spectrum contains multiple peaks over the frequency range 2-20MHz. The majority of these peaks lie in the 2-10MHz region, but there is a distinct spectral feature associated with the presence of a defect around 15MHz (identified using a green circle), which offers potential for defect analysis. Furthermore, for the specific A-scan signals identified in FIGURE 5, the calculated frequency spectra are presented in FIGURE 6. It can be clearly seen that the spectral peaks in the 2-10MHz range are reasonably consistent between these two signals and the frequency component around 15 MHz demonstrates a different characteristic from the no defect case. Therefore, this

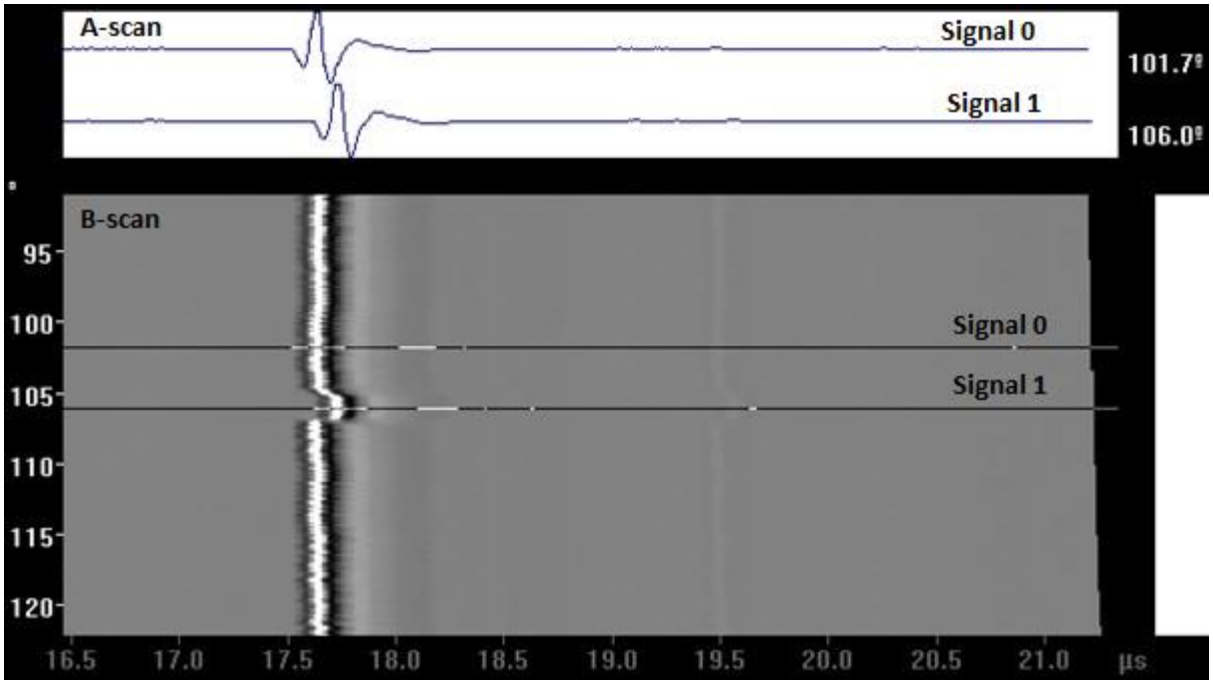

FIGURE 4. An example of well-focused ultrasonic signals presented using the FLAW analysis package

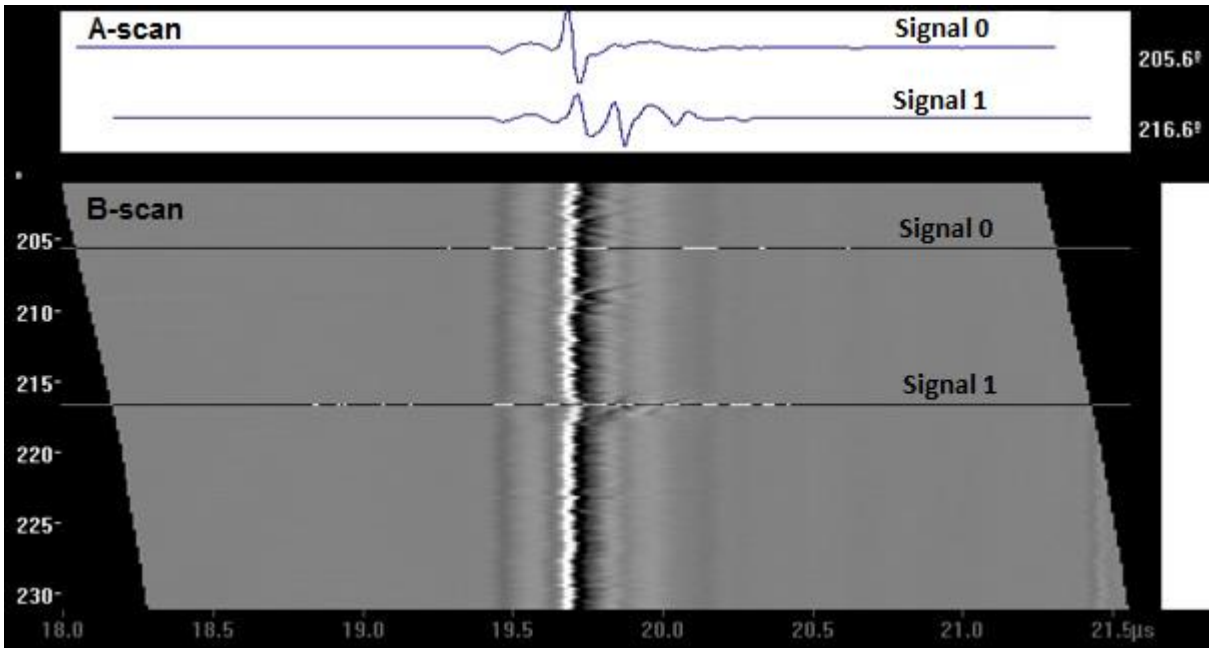

FIGURE 5. An example of poorly-focused ultrasonic signals presented using the FLAW analysis package

suggests that filtering of the spectral content may lead to the generation of useful information in terms of the defect response.

Wavelet decomposition can be considered as applying groups of low pass and high pass filters to the signal of interest, with the group number dependent on the number of decomposition levels. After convolving the A-scan signal with the Haar wavelet, the coefficients can be used to reconstruct the approximation and detail separately. The two A-scan signals (*S*) from FIGURE 5 are used as an example to demonstrate this processing approach. The approximation (*A2*) and detail signals (*D1* and *D2*) are presented in FIGURE 7. From the decomposed signals, the detail signal on level 1 (*D1*) is identified as containing defect information due to the high frequency signal extracted from the inspection data. Unfortunately, the second level detail and approximation signals contain significantly less information of the defect, as observed from the Figure. There

are two peaks in the detail signal with defect on level 1 (*D1*). The first peak indicates the echo information from the near tube surface while the second one is an indication of the defect bottom.

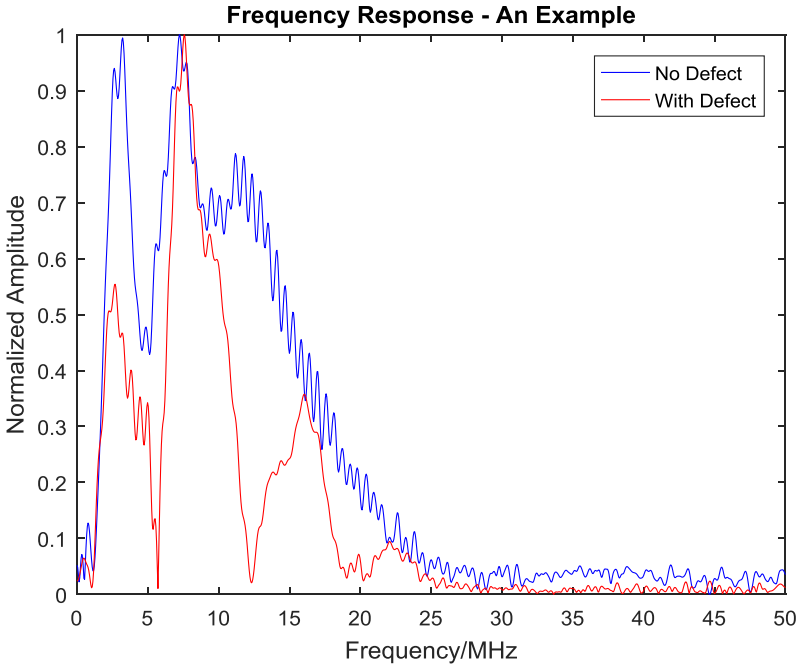

FIGURE 6. Frequency response of for A-scans from a no defect (Signal 0) and defect (Signal 1) regions from FIGURE 5

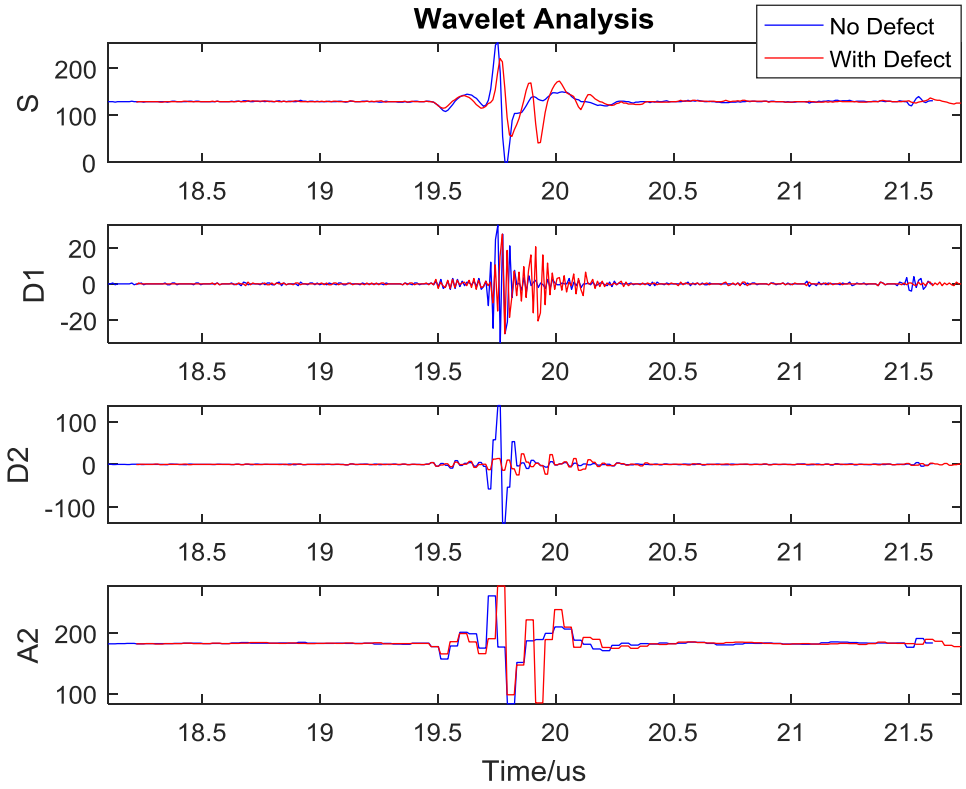

FIGURE 7. Wavelet analysis of no-defect signal and with-defect signal; S: original signal, D1: detail signal on level 1, D2: detail signal on level 2, A2: approximation signal on level 2

4. RESULTS AND DISCUSSION

4.1 Results

As a result of the application of wavelet analysis, shown in FIGURE 7, the low frequency information has effectively been filtered out and the high frequency components utilized to highlight the temporal characteristics of the defect in signal *D1*. FIGURE 8(a) displays the original A-scan signals and the corresponding wavelet analysis results. Additional processing of these waveforms generates the envelope representations, as presented in FIGURE 8(b). The original time domain signal from the defect, identified as red line in FIGURE 8(a), poses significant challenges in selecting which peak accurately represents the defect depth. Whereas, the peaks in the envelope signal, presented in FIGURE 8(b), can be clearly identified and used to calculate the defect depth. Subsequently, the depth calculation produced a depth 0.1136mm. The original verified estimate of this defect depth from an experienced Analyst was 0.12 mm. Hence, there is a measurement error of about 5% in this case, which is well within the expectation that defect depth errors should be within 0.04 mm. In order to evaluate this approach further, 46 data acquisitions from 8 pressure tube scans have been selected and subjected to this wavelet analysis approach. Importantly, 38 out of the 46 now show improved defect detection and importantly, defect depth calculations within the expected error range. TABLE 1 compiles the results from 20 datasets, presenting defect depth measurement results and the corresponding errors as compared to the verified results generated by an Analyst.

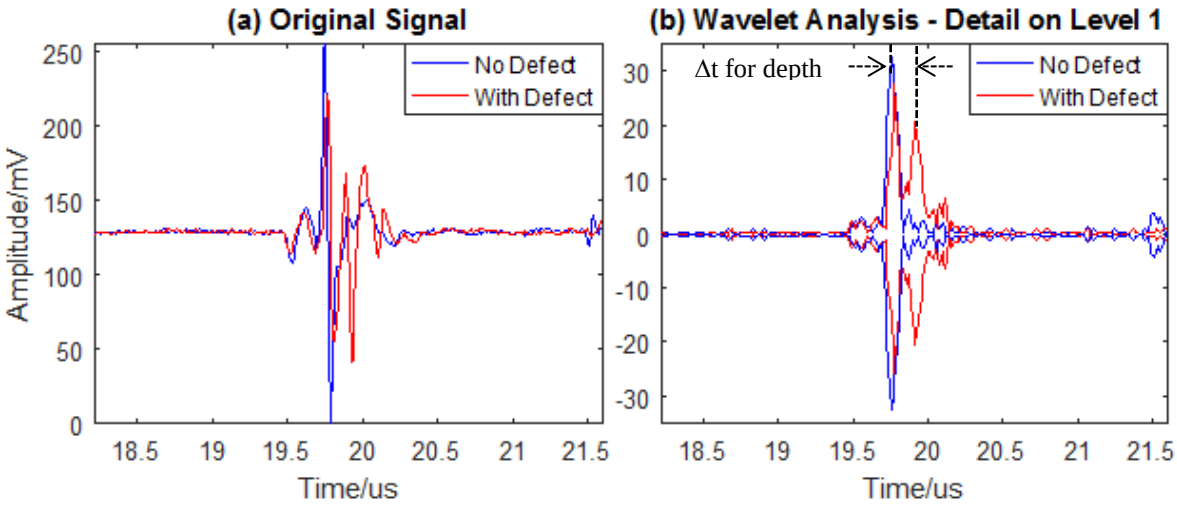

FIGURE 8. Original A-scan signals and envelopes of wavelet analysis detail signals on level 1 (no-defect signal and with-defect signal respectively)

TABLE 1. Defect depth measurement results and errors

No.	Dataset Name	Defect Position (mm)	Wavelet Analysis Result (mm)	Verified Results (mm)	Errors (mm)
1	A1241 C07 (2944-2955)	2949.2	0.2911	0.28	0.0111
2	A1241 C07 (3752-3763)	3756.8	0.1704	0.18	0.0096
3	A1241 C07 (6321-6329)	6325.4	0.1349	0.14	0.0051
4	A1241 D15 (7381-7419)	7412.4	0.0852	0.12	0.0348
5	A1241 D15 (8322-8562)	8474.4	0.1136	0.1	0.0136
6	A1241 G12 (2568-2607)	2576.8	0.1136	0.13	0.0164
7	A1241 G12 (4126-4135)	4130.0	0.1349	0.11	0.0249
8	A1241 G12 (5440-5449)	5445.2	0.3408	0.32	0.0208
9	A1241 Q14 (2838-2849)	2844.2	0.2698	0.28	0.0102

10	A1241 Q14 (4593-4620)	4612.6	0.2201	0.23	0.0099
11	A1241 Q14 (8606-8657)	8618.4	0.1136	0.12	0.0064
12	A1431 D16 (5847-5857)	5851.4	0.3763	0.38	0.0037
13	A1431 D16 (5869-5878)	5873.2	0.1278	0.16	0.0322
14	B1381 D17 (3152-3155)	3153.0	0.1278	0.12	0.0078
15	B1381 D17 (4302-4305)	4303.0	0.0994	0.11	0.0106
16	B1381 D17 (4478-4484)	4479.6	0.1136	0.11	0.0036
17	B1561 C14 (3690-3700)	3694.2	0.142	0.11	0.032
18	B1561 C14 (4973-4983)	4976.2	0.2414	0.21	0.0314
19	B1561 N10 (8715-8722)	8717.2	0.1562	0.15	0.0062
20	B1561 N10 (5659-5670)	5662.2	0.1349	0.11	0.0249

4.2 Discussion

The selection of the wavelet used for signal processing is a compromise between time resolution and frequency resolution. By applying the Haar wavelet, a good time resolution can be obtained which is suitable for the requirement of measuring small defect depths. The transfer function of Haar filter on level 1 is presented in FIGURE 9 and illustrates the low frequency filtering effect as a gradual process as opposed to a rapidly changing characteristic, for example. Importantly, in the current implementation, the frequency resolution is sacrificed. Therefore, an alternative wavelet could be considered in the future to maintain a better time and frequency balance.

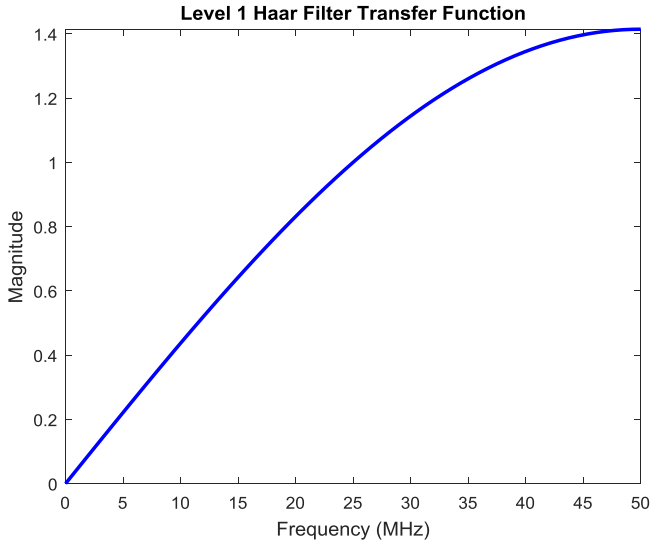

FIGURE 9. Transfer function of Haar filter on level 1

5. CONCLUSION

A wavelet analysis method of extracting defect depth information from poorly-focused A-scan signals associated with pressure tube inspection is proposed in this paper. The spectral characteristics associated with ultrasonic echoes from the pipe wall and the defect have similarities in the low frequency range (2-10MHz), but the defect signal has a distinct spectral peak around 15MHz. A Haar wavelet approach has been adopted to exploit this difference in the frequency domain, whilst maintaining good temporal accuracy. Results on 48 datasets demonstrate the success of this signal processing approach, with good agreement between the processed

defect depth and the reported defect depth by an experienced Analyst in over 80% of cases. It is envisaged that utilization of this advanced processing method could improve depth measurements from poorly focused A-scan datasets and thereby save on the cost of further inspection processes, for example precision depth measurement from replicas.

ACKNOWLEDGEMENT

The authors would like to thank the studentship sponsored by Duncan Hawthorne Scholarship for funding of Huan Zhao's PhD.

REFERENCES

1. M. Trelinski, "Ultrasonic Testing Methods and Procedures for Volumetric and Surface Inspection of CANDU Reactor Pressure Tubes," presented at the European Conference on Non-Destructive Testing, Berlin, 2006.
2. C. H. Frazier and W. D. O'Brien, "Synthetic Aperture Techniques with a Virtual Source Element," *IEEE Transactions on Ultrasonics, Ferroelectrics, and Frequency Control,* vol. 45, p. 12, 1998.
3. M. Wuest, M. Nierla, and S. J. Rupitsch, "A Model-based Synthetic Aperture Focusing Technique for Acoustic Microscopy," in *2016 IEEE International Ultrasonics Symposium Proceedings*, 2016, p. 5.
4. S. C. Her and S. T. Lin, "Non-Destructive Evaluation of Depth of Surface Cracks Using Ultrasonic Frequency Analysis," *Sensors (Basel),* vol. 14, pp. 17146-58, 2014.
5. G. K. Sharma, A. Kumar, C. Babu Rao, T. Jayakumar, and B. Raj, "Short Time Fourier Transform Analysis For Understanding Frequency Dependent Attenuation In Austenitic Stainless Steel," *NDT & E International,* vol. 53, pp. 1-7, 2013.
6. C. J. Pritchard and P. Rubbers, "An Overview of Split Spectrum Processing," *The e-Journal of Nondestructive Testing,* vol. 8, 2003.
7. T. Bouden, F. Djerfi, and M. Nibouche, "Adaptive Split Spectrum Processing for Ultrasonic Signal in The Pulse Echo Test," *Russian Journal of Nondestructive Testing,* vol. 51, pp. 245-257, 2015.
8. M. Ruzzene, "Frequency-Wavenumber Domain Filtering for Improved Damage Visualization," *Smart Materials and Structures,* vol. 16, pp. 2116-2129, 2007.
9. T. E. Michaels, J. E. Michaels, and M. Ruzzene, "Frequency-Wavenumber Domain Analysis of Guided Wavefields," *Ultrasonics,* vol. 51, pp. 452-66, 2011.
10. S. P. Song and P. W. Que, "Wavelet Based Noise Suppression Technique and Its Application to Ultrasonic Flaw Detection," *Ultrasonics,* vol. 44, pp. 188-93, 2006.
11. W. Liang and P.-w. Que, "Optimal Scale Wavelet Transform for The Identification of Weak Ultrasonic Signals," *Measurement,* vol. 42, pp. 164-169, 2009.
12. Y. Wang, "Wavelet Transform Based Feature Extraction for Ultrasonic Flaw Signal Classification," *Journal of Computers,* vol. 9, 2014.
13. I. Daubechies, *Ten Lectures on Wavelets*: Society for Industrial and Applied Mathematics, 1992.